Lignin solvation by ionic liquids: the role of cation

Jon Zubeltzu[a,b,c], Elena Formoso[b,d], Elixabete Rezabal[a,b]

[a] *Kimika Fakultatea, Euskal Herriko Unibertsitatea (UPV/EHU), 20018 Donostia, Euskadi (Spain)*
[b] *Donostia International Physics Center (DIPC) 20018 Donostia, Euskadi (Spain)*
[c] *Ingenieritza Fakultatea, Euskal Herriko Unibertsitatea (UPV/EHU), 20018 Donostia, Euskadi (Spain)*
[d] *Farmazia Fakultatea, Euskal Herriko Unibertsitatea (UPV/EHU), 01006 Vitoria-Gasteiz, Euskaldi (Spain)*

Abstract

The use of ionic liquids as solvents for the processing of lignocellulosic material has received considerable attention in the last years, since it presents remarkable advantages over previous solvent-based procedures. In particular, their ability to dissolve and treat the lignin has become of major interest lately. Liquid salts at room temperature, ionic liquids have unique physicochemical properties as compared to conventional solvents, due to the interactions they can establish among ions and with other solutes. From the theoretical chemistry point of view, the correct description of these interactions in a dynamic environment requires computationally demanding methodologies, and therefore settling for a certain theoretical level requires invariably a compromise between accuracy and computational cost. In this article we present a detailed analysis of the interactions established by commonly used ionic liquids with the lignin, with special focus on the role of the cation, motivated by the discrepancies arising from literature. A multiscale simulation strategy, including static and dynamic density functional theory and molecular dynamics calculations, has permitted to provide a reliable, multifaceted description of the solvation pattern of lignin, reporting for the first time the dual role of imidazolium-based cations stabilizing both the hydroxyl groups and aromatic rings of the lignin.

Keywords: Ionic liquids, lignin, ab initio molecular dynamics, density functional theory

Email address: elixabete.rezabal@ehu.eus (Elixabete Rezabal)

1. Introduction

The use of lignocellulosic biomass as a primary source for obtaining the chemical compounds that sustain our way of living is being intensively studied during the last years. Lignocellulosic biomass is composed of two polysaccharides, cellulose and hemicellulose, and an aromatic polymer, lignin. Traditionally, most interest has been focused on cellulose, while lignin has been treated as waste product. Recently, however, the recovery and use of one of the most abundant renewable aromatic polymers has become a relevant challenge for the scientific community, as a crucial step for ensuring the economic viability of biorefineries [1, 2, 3]. The transformation of biomass into valuable molecules is a complex process that requires the separation of the raw biomass into its polymeric components for their subsequent dissolution, extraction and depolimerization [4, 5]. Ionic liquids (ILs) have been reported to perform efficiently in the different steps of the process, both for cellulose and lignin [1, 6, 7, 8], overcoming the limitations other strategies present.

ILs are salts whose melting temperature is around or below the room temperature, and they are usually formed by an inorganic anion, and an organic cation. The nature of the selected ions determines the physicochemical properties of the material, and therefore, each IL shows a diverse ability to dissolve the different parts of the lignocellulosic biomass. There is a massive amount of possible combinations, and in the last years, scientists have tried to elucidate the role of each constituent on its final performance [9]. This task becomes highly complicated when it comes to lignin; besides its intrinsic structural heterogeneity and variability, it undergoes several chemical modifications throughout the process, making experimental results highly dependant on the particular type of lignin and process employed [3]. Consequently, the basic features of the lignin-IL interactions, upon which the whole dissolution, depolimerization and processing rely, are still not well understood.

The theoretical chemistry community has also contributed to this effort; most theoretical works study this type of systems by using density functional theory (DFT), considering only one lignin monomer (represented by a small model) and one or two molecules of IL, either in gas phase [10, 11] or surrounded by implicit solvent [**?** **?**]. Including the influence of the liquid environment proved to be crucial to reproduce the experimental results in

the work by Sun et al., where the solvation of dilignol models by cholinium and imidazolium based ionic liquids was addressed [13]. Accordingly, Janesko included the influence of an aqueous environment by means of the Solvation Model based on Density (SMD) for analyzing the interaction of imidazolium-based ILs with the monolignol unit [**?**], and the generalized SMD for ILs (SMD-GIL) [14] in a posterior work [**?**], devoted to analyzing the depolymerization of lignin by ILs. Even though initially it was suggested that the anion has a dominant role in the solubilization of lignin [15, 11, 16], recent works employing DFT [10] suggest that the picture is rather complex and both anion and cation contribute to the process, even if the role of the latter is still unclear [17]. In particular, Janesko suggested that the cation contributed to the solvation of lignin via π stacking interactions in the case of imidazolium-based interactions [**?**], on the contrary to experimental works indicating the side chain modulates the affinity for lignin [17, 18, 19].

The static DFT calculations performed so far on the solvation of lignin by ILs provide an accurate representation of the interactions present in the system. However, they are limited by their lack of ability to capture the fluctuating nature of liquid environments. A possibility to noticeably improve the representation of these interactions is to include explicitly the molecules of the solvent and carry out molecular dynamics (MD) calculations for such type of system. Indeed, some groups have studied the lignin solvation by explicit IL ion pairs, by means of classical MD calculations, providing an atomic level description of the system, based on parameterized force fields. Employing those methods, Moyer and coworkers [17] analyzed the solvation ability of selected ILs and compared the results with experimental data. They observed that, even if both type of ions take part in the solvation of the lignin, the characteristics of the anion do not correlate with the experimental solvation ability of the liquid. Zhu et al. [20], choosing a similar methodology, provide a more detailed description of the lignin solvation in an imidazolium-based IL: apart from reporting a π-π interaction between the imidazolium ring and the lignin in agreement with Janesko et al. [**?**], they include the formation of H bonds between the cation ring hydrogens with the lignin hydroxyl group and ring π system.

Even if these classical MD techniques provide statistically significant trajectories of big systems at a reasonable computational effort, they have limitations in correctly representing intermolecular interactions that are the basis of IL physicochemical properties, as dispersion and charge transfer interactions. The adequate representation of such interactions can be obtained by

the much more computationally demanding ab initio MD (AIMD) methods (not yet considered in the literature for the lignin-IL system), which provide an electronic level description of the system, based on DFT, at a much higher computational cost. As a consequence, the accumulation of sufficient statistical sampling and thus, the dependence of the results on the initial geometry chosen is a limitation of these methods. Therefore, considering that classical and ab initio MD contributions provide complementary insights into the system under study, the present work aims to tackle the solvation pattern of lignin from a multiscale perspective, assessing and overcoming the limitations of each particular method. These dynamic simulations will be complemented with static, cluster-continuum representations of the solvation process.

Among the vast choice of ILs available, we have chosen to study an imidazolium based IL, which are the most widely used and studied type of IL. In particular, we considered the butyl-methylimidazolium chloride ([BMIM][Cl]) (see Figure 1 (a)), known to be capable to dissolve both cellulose and lignin simultaneously [21]. Recently, [BMIM][Cl] was reported to efficiently dissolve and depolymerise lignin from corn stover [22]. Furthermore, [BMIM][Cl] is a particularly interesting IL to study from a computational chemistry point of view, since each type of ion interacts with neutral organic molecules in a distinct manner: dispersion interactions are established by the cation, and dipole-charge interactions by the anion [23, 24]. Therefore, this IL does not only permit the separation of the role of each ion, but also the influence of each type of interaction. Special attention will be payed to the role of the cation, which is still a matter of debate in the literature. Finally, since the melting temperature of this IL (342 K [25]) limits its interest from the experimental point of view, the last part of this paper is devoted to experimentally more relevant materials, and their performance as lignin solvents is discussed in terms of the interactions they are able to establish with the solute.

2. Computational details

In order to keep DFT based calculations within an acceptable computational cost, lignin is represented in this work as a monolignol model (see Figure 1 (b)), in consonance with the other DFT studies in the literature [**?** 16]. For the sake of consistency, the same model is considered in all the different theoretical approaches employed in the study. The use of small models to represent lignin implies a significant approximation to the real system, but has also two remarkable advantages: firstly, it considerably reduces the com-

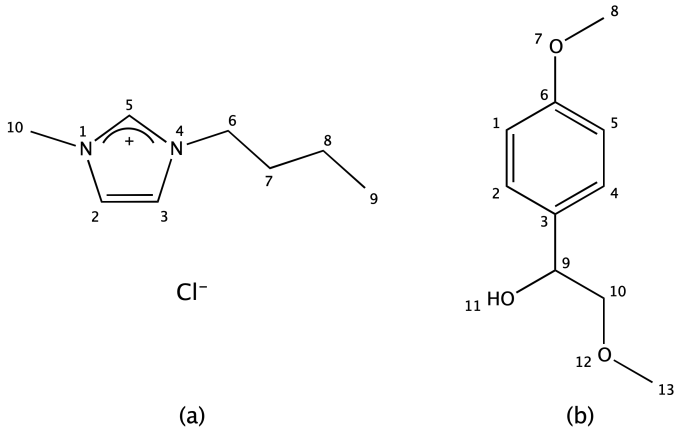

Figure 1: Chemical structures of the (a) ionic liquid butyl-methylimidazolium chloride, [BMIM][Cl], and (b) lignin model used, together with the numbering used throughout the text

putational cost of the calculations. Secondly, given the intrinsic variability of the lignin structure and the difficulty of its experimental characterization, we can focus on the basic moieties of the polymer that provide fundamental information of the interactions between selected parts of the lignin and the ILs. The latter is specially important given that these interactions are known to have relevance not only in the dissolution step, but also during the whole transformation process of lignin, as the depolimerization.

For the sake of clarity, the atom numbering of the lignin model and the $BMIM^+$ cation presented in Figure 1 will be used throughout this work for referring to the atoms, specifying first the molecule the atom belongs to, then the type of atom, and finally its position in the molecule. For example, ^{lig}O11 refers to the O atom in position 11 of the lignin molecule, as numbered in Figure 1.

The classical MD calculations were carried out by the LAMMPS code [**?**]. The interactions of the lignin molecule were modeled by the OPLS-AA force-field [**?**], while the interactions of the IL were represented by a recently parameterized force-field by Mondal et al. [26]. The initial configuration of the molecules within the simulations box was obtained by randomly placing 160 pairs of IL molecules and a single lignin molecule by the Packmol package [**?**]. The SHAKE algorithm was applied during the integration of the equations of motion of the stretching terms of the bonds that include a hydrogen atom. The long-range interactions were computed by the particle-particle

particle-mesh algorithm (PPPM) [**?**] and a timestep of 2 fs was set. During the first 1 ns of the run, the NPT ensemble was adopted by applying the Parrinello-Rahman [**?**] barostat keeping the cubic shape of the simulation cell. Thereby, an equilibrium value of the volume at P = 1 atm and T = 373 K was obtained, with a density of 1.005 g/cm^3. Then, the NVT ensemble was used at T = 373 K for 10 ns for the correct thermal equilibration of the system followed by 10 ns of production run.

AIMD simulations were produced at the same temperature based on the Born-Oppenheimer approach as implemented in the Quickstep code of the CP2K software [27]. The functional used was BLYP[32, 33**?**], with D2 dispersion correction by Grimme [**?**], combined with DZVP-MOLOPT-SR-GTH basis sets [**?**]. Two production runs of around 95 ps were obtained, starting from two different geometries extracted from the classical MD simulation, in order to attenuating the influence of the initial geometry in the AIMD results. In these calculations, the monolignol model was surrounded by 20 IL ion pairs. The high computational cost of AIMD calculations in comparison to classical MD simulations makes the accumulation of a sufficient statistical sample a limiting factor of this theoretical approximation. The simulation time required for the system to converge starting from arbitrary geometries was estimated by carrying out classical MD simulations with the same set up as AIMD calculations, namely a box of 20 IL pairs and a time step of 0.5 fs. In these simulations, the ^{lig}H11-Cl$^-$ interaction, consistently reported to be a stable interaction in the literature, shows no significant variation from 90-100 ps on, besides the exchange of the anion with the bulk, which is not the scope of the present paper (see Supplementary Material). Consequently, AIMD runs of this time length were considered to be reliable enough for studying the solvation pattern of lignin in the selected IL.

The distribution of the ions around the lignin in both ab initio and classical MD calculations was analyzed by means of radial distribution functions (RDFs) computed with the TRAVIS trajectory analyzer [28]. The radial distribution function or g(r) gives the distribution of the density with respect to distance around a referential particle. Therefore, it provides structural information around the particle of interest. Additionally, a topological analysis of the electronic density of the IL-lignin interactions throughout the dynamic calculations was performed by the average Non Covalent Index method (aNCI) as implemented in the NCIplot software[29, 30].

Finally, static DFT calculations were performed by means of the Gaus-

sian software [31]. Following a cluster-continuum approach, three IL pairs of ions were explicitly included in the coordination shell of lignin, and the rest of the solvent was modeled by an implicit continuum. For the latter, the SMD-IL model [14] was employed, whose parameters were adjusted to fit the characteristics of each IL. The structures were optimized and their frequencies calculated to guarantee the stationary nature of the obtained geometries. Several local energy minima were characterized for each IL at the B3LYP/SVP [32, 33, 34, 35] level corrected with Grimme's dispersion correction [36], among which the global minimum will be considered for discussion (see Supplementary Material). Energies were refined by M062X/TZVP [37, 38, 35] single point calculations. The affinity of the IL with the lignin was estimated as the electronic energy difference between the optimized monolignol-IL complex and the infinitely separated monolignol and IL ion pairs system. The latter was obtained by maintaining the optimized geometry of the complex.

3. Results and discussion

3.1. Molecular dynamics study

The RDF of the Cl^- anions around the lignin obtained from the classical MD trajectory reveals, as expected, a sharp first neighbour peak, suggesting that they interact preferentially with the hydroxyl group of the lignin via its ^{lig}H11 atom (see Figure 2(a)). The maximum of the RDF is found at around 190 pm, and the first minimum at 340 pm. Although this minimum is quite low, is not strictly zero, which indicates that there is an exchange of Cl^- anions between the first solvation shell and the bulk.

Regarding the participation of the cations on the solvation of the lignin molecule, the overall picture shows a rather weak organization of the cations around the lignin. The interactions between ^{imi}H2-5 and ^{lig}O11 or π system of the lignin reported in the literature [20] were not observed; RDFs show no significant correlation between the ^{imi}H2-5 atoms and ^{lig}O11 (see Figure 2(b)). Furthermore, there is no indication of a π-π interaction between the imidazolium ring and the solute, but rather some structuration of the cation side chain (in particular the terminal ^{imi}C9 carbon) around the lignin ring at 500 pm (see Figures 2(c) and (d)).

Aiming for an improved description of the interactions established between the IL and lignin, ab initio MD calculations were performed starting

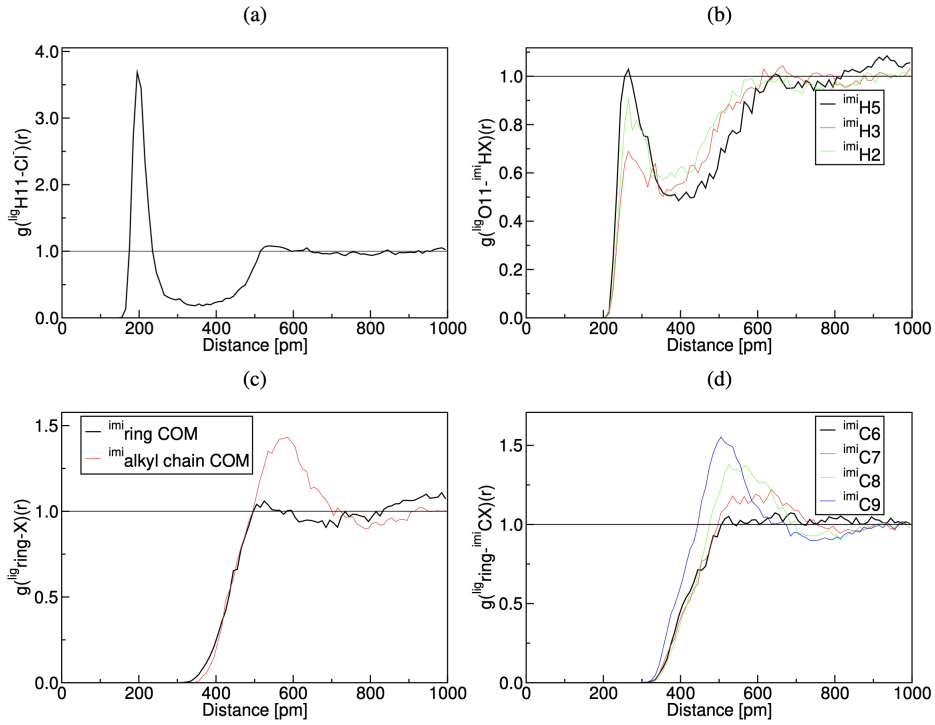

Figure 2: Radial distribution functions obtained from the classical MD simulations between several atomic species: (a)^{lig}H11 - Cl^-, (b) ^{lig}O11 - ^{imi}H5, ^{lig}O11 - ^{imi}H3 and ^{lig}O11 - ^{imi}H2, (c) ^{lig}ring COM-^{imi} ring COM and ^{lig}ring COM-^{imi} alkyl side chain COM, and (d) ^{lig}ring COM-^{imi}C6, ^{lig}ring COM-^{imi}C7, ^{lig}ring COM-^{imi}C8 and ^{lig}ring COM-^{imi}C9. COM stands for center of mass.

from two different configurations extracted from the classical MD trajectory. Overall, both AIMD trajectories indicate very similar solvation pattern of the lignin. For the sake of brevity, only one of the AIMD trajectories (named AIMD1) will be discussed throughout the document; the structural and topological analysis of the other trajectory (named AIMD2) is available as Supplementary Material.

As expected, a very localized peak at around 206 pm (see Figure 3(a)) is found in the ^{lig}H11-Cl^- RDF, which decreases to 0 at around 280 pm, indicating no exchange of chlorine anions with the IL during the first 95 ps. In line with classical MD calculations, the AIMD calculations do not show a π-π interaction between imidazolium and lignin rings, as reported in the literature, but rather a structuration of the aliphatic chains of the cation around the lignin ring, in particular carbons ^{imi}C8 and ^{imi}C9 at 375 pm (see

Figures 3 (c) and (d)). In fact, if the evolution of the ^{lig}ring-^{imi}ring RDF of AIMD1 is analyzed in 10 ps intervals (see Figure S4), we can observe that the ^{lig}ring-^{imi}ring interaction has indeed been explored between 10 and 40 ps, for then losing relevance during the remaining 55 ps. Finally, on the contrary to classical MD simulations, AIMD calculations do report a significant correlation between a H atom of the imidazolium molecule and ^{lig}O11 (see Figure 3(b)) at around 230 pm. Nevertheless, instead of ^{imi}H2 and ^{imi}H3 reported by Zhu et al., in our case the most acidic proton, ^{imi}H5, is the one which interacts more strongly.

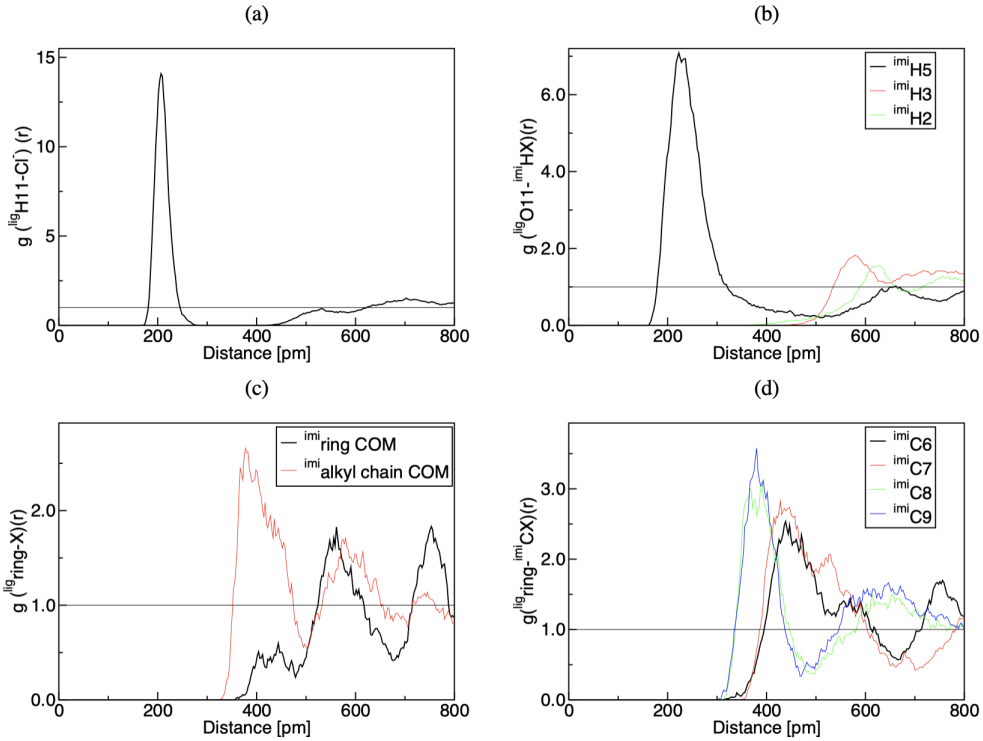

Figure 3: Radial distribution functions obtained from AIMD calculations between several atomic species: (a)^{lig}H11 - Cl^-, (b) ^{lig}O11 - ^{imi}H5,^{lig}O11 - ^{imi}H2, ^{lig}O11 - ^{imi}H3, (c) ^{lig}ring COM-^{imi} ring COM and ^{lig}ring COM-^{imi} side chain COM, and (d) ^{lig}ring COM-^{imi}C6, ^{lig}ring COM-^{imi}C7, ^{lig}ring COM-^{imi}C8 and ^{lig}ring COM-^{imi}C9. COM stands for center of mass.

The nature of the interactions was analyzed by means of the aNCI method [29, 30] (see Figure 4), already successfully applied on similar systems [24]. The analysis shows two type of interactions between the lignin and the IL: i)

a localized, strong hydrogen bond interaction with the hydroxyl group (blue surface in Figure 4(a)), and ii) dispersed, non directional London interactions with the ^{lig}O11 (see Figure 4(a)) and aromatic ring (see Figure 4(b)), represented as wide green surfaces. These interactions correspond precisely to i) the ^{lig}H11 - Cl^- bond and ii)^{lig}O11 - ^{imi}H5 and ^{lig}ring -^{imi} side chain interactions identified in the RDFs in Figure 3.

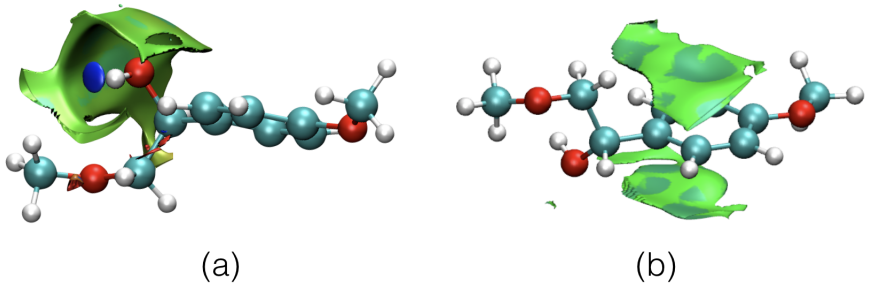

Figure 4: aNCI analysis of the interactions established by (a) ^{lig}H11 (localized, blue surface close to the hydrogen, sign(λ_2)ρ = -0.038) and ^{lig}O11 (wide green surface around the oxygen atom, $\rho \simeq 0.012$) and (b) ^{lig}ring (wide green surface above and below the ring, $\rho \simeq 0.014$) with the surrounding IL within a radius of 4 Å

.

In summary, ab initio and classical MD simulations overall show a similar solvation picture of lignin: the strongest interaction is the one between the hydroxyl and the anion, while the rest of the molecule establishes dispersion interactions with the cations. In particular, both theoretical description levels suggest a preference of ^{lig}ring for the alkyl chain of the imidazolium cation as compared to the imidazolium ring. AIMD calculations predict overall stronger dispersion interactions than classical MD calculations; this is evident when comparing the ^{lig}ring-^{imi}alkyl chain RDFs in Figures 2(d) and 3(d); the former presents its maximum at around 500 pm while the second is found at around 375 pm. The difference is specially evident when regarding the ^{lig}O11-^{imi}H5 interaction, which the AIMD calculations are able to capture while the classical MD calculations are not. While this could in part be due to the limited statistical sampling and consequent influence of the initial geometry on AIMD, the fact that very similar results are obtained for both AIMD1 and AIMD2 trajectories, and the observation of the evolution of the RDFs suggest that a reasonable amount of statistical sampling has been accumulated.

These discrepancies between both methods are directly related to their intrinsic limitations, exposed in the introduction of this work. In order to assess the description of the interactions in our system by the different theoretical approximations, we performed a set of scans in a small model system consisting of the lignin monomer and a [BMIM][Cl] ion pair. We considered the different interactions found between the solute and IL, namely the ^{lig}H11-Cl$^-$ interaction, the ^{lig}ring-^{imi}side chain interaction, and the ^{lig}O11-^{imi}H5 interaction; besides, the ^{lig}ring-^{imi} ring interaction suggested in the literature but not found in our calculations was also included. A scan along these interactions was carried out employing the theoretical levels considered throughout this study, namely the forcefield and BLYP-D/DZVP-MOLOPT-SR-GTH, (see Figure 5). As expected, ^{lig}H11-Cl$^-$ bonds are well captured by classical MD even if the minimum is found at shorter distances as compared to DFT (1.8 Å vs 2.0 Å), in agreement with the RDFs analyzed in Figures 2(a) and 3(a). On the contrary, the interactions between the cation and lignin are overall not properly accounted for by the force-field, since very shallow minima are found in the scans at remarkably longer bond distances as compared to static DFT. These interactions were identified as dispersion interactions by aNCI analysis, and therefore this indicates the limitations of our classical MD approximation to capture the dispersion interactions of the system, and consequently, the role of the imidazolium-based cations in solvation processes. AIMD calculations, on the contrary, do describe correctly the dispersion interactions, as a consequence of Grimme's correction term included in the model, which was previously assessed to be key for obtaining reliable results in a very similar system [23]. Therefore, the discrepancy between both approaches in describing the ^{lig}O11-^{imi}H5 interaction, and, to a lesser extent the ^{lig}ring COM-^{imi}C9 structuration, is most likely related to the limitations of the classical MD simulations.

3.2. Influence of the ion nature

The experimental requirements of working with [BMIM][Cl] limit its applicability to real systems, making other ion combinations much more attractive. Therefore, having identified the basic interactions taking place in lignin solvation, the influence of the identity of the ions forming the IL was analyzed. The aim is not to describe the solvation pattern of lignin in these alternative combinations, but rather to have an indication of how the affinity of the IL for the lignin would change if other ions were considered.

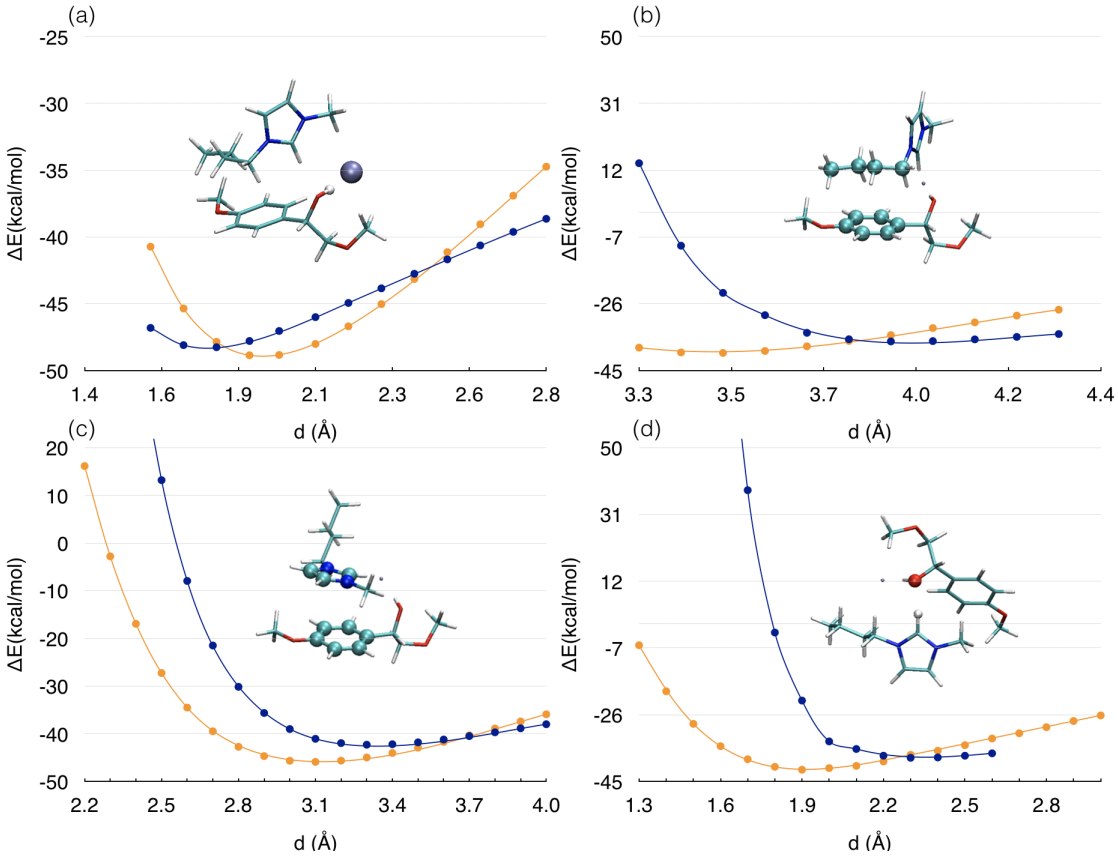

Figure 5: Scans of the different lignin-IL interactions considered in the study: (a) ^{lig}H11-Cl$^-$ bond (b) ^{lig}ring -^{imi}alkyl side chain (c) ^{lig}ring -^{imi}ring (d) ^{lig}O11-^{imi}H5 interaction. Blue dots stand for the force-field-based calculations and orange ones for BLYP-D/DZVP-MOLOPT-SR-GTH. The images correspond to the local minima characterized for each interaction; the atoms or groups of atoms among which the distance was scanned are indicated as spheres in each case. ΔE is calculated as the electronic energy difference with the infinitely separated fragments.

Two experimentally widely used cations and anions were chosen and compared to BMIM$^+$ and Cl$^-$. Namely, Et_3NH^+ and choline (2-Hydroxy-N,N,N-trimethylethan-1-aminium) were chosen; the latter is particularly interesting, since it is an essential nutrient. Regarding the anions, the performance of acetate (also experimentally observed to be efficient in lignin dissolution and extraction [39]), and $CH_3SO_4^-$ were compared to Cl$^-$. All the combinations of these ions are considered (the characterized global minima are presented

in Figure 6, while the rest of characterized structures are in Supplementary Material), with the aim of systematically assessing the affinity differences when altering the physicochemical characteristics of the ion.

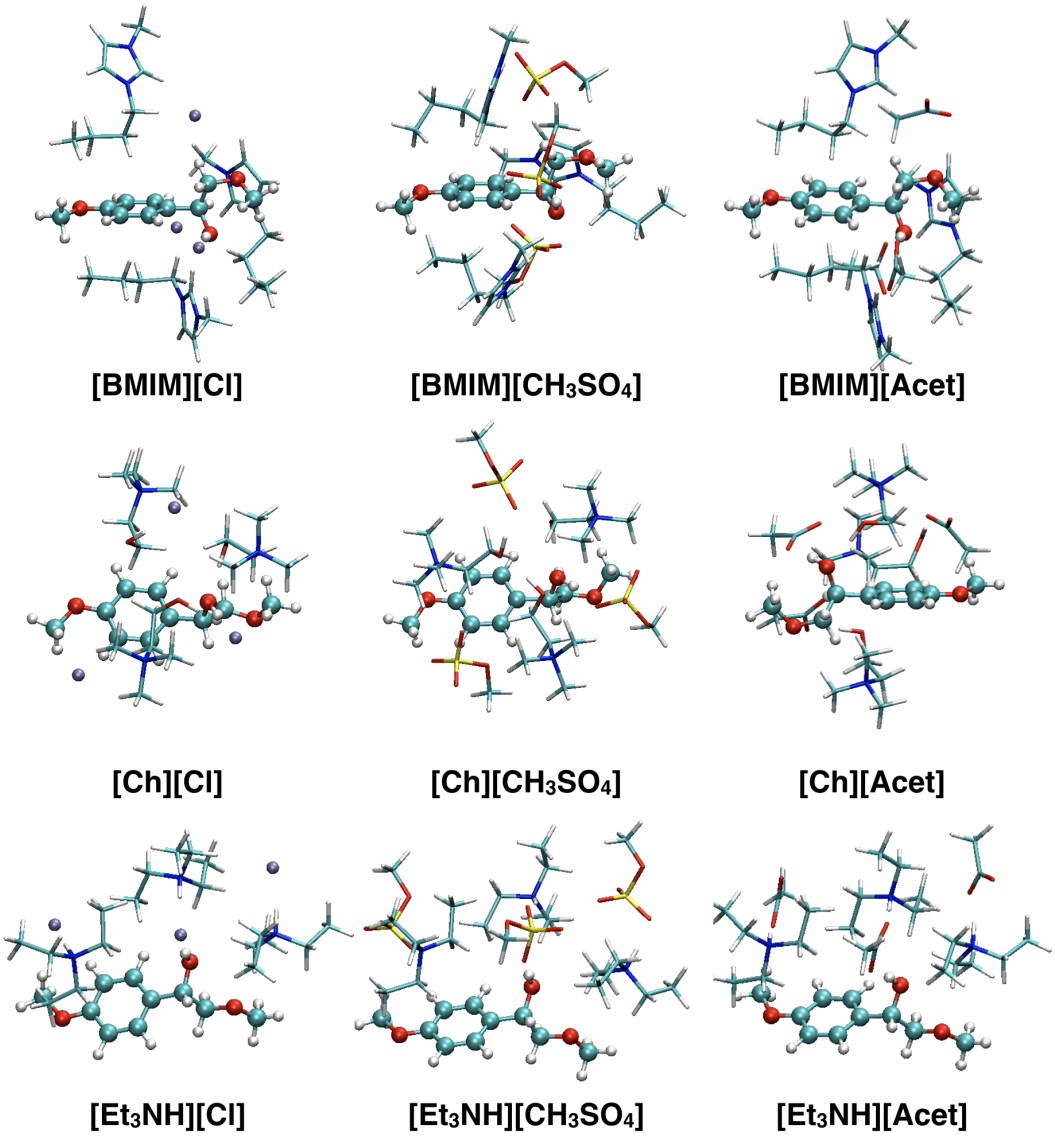

Figure 6: IL-lignin global minima characterized at the B3LYP-D/SVP(SMD) level. Ch stands for choline cation in this figure.

The calculated affinities (see Table 1) point out that the binding energy

	Cl^-	$CH_3SO_4^-$	$Acet^-$
$BMIM^+$	-28.9	-30.8	-29.8
Et_3NH^+	-15.1	-14.3	-15.6
Ch^+	-23.0	-26.5	-27.3

Table 1: Binding M062X/TZVP//B3LYP-D/SVP(SMD) enthalpies, in kcal/mol.

is dominated mainly by the nature of the chosen cation; $BMIM^+$ based ILs show the strongest affinity for the lignin (between -28.9 and -30.8 kcal/mol), followed closely by choline based ILs (between -23.0 and -27.3 kcal/mol) and Et_3NH^+ based ILs, which show a much lower affinity (between -14.3 and -15.6 kcal/mol). The anions have a smaller influence, without a clear trend in the variation of the affinity with the anion nature. The affinity varies up to 2 kcal/mol for the $BMIM^+$ and Et_3NH^+ based ILs, while the choline chloride IL shows an affinity up to 4 kcal/mol smaller than the other choline combinations.

The coordination pattern found in these complexes is overall in agreement with the MD study presented in the first part of this work: $BMIM^+$ and Et_3NH^+ establish only dispersion interactions with the lignin thanks to the alkyl chains, and, consequently, $BMIM^+$ based ILs show a better affinity for the lignin, since its side chain is bigger in size than Et_3NH^+, which has three ethyl chains. Choline, on the other hand, can establish hydrogen interactions with its hydroxyl group in addition to dispersion interactions with the alkyl groups, and therefore, its affinity is comparable to that of $BMIM^+$ despite its small size.

Regarding the anions, the influence of the nature of the anion is much weaker than that of the cation, probably because in the complexes under study all of them establish a very similar anion-hydroxyl interaction and the influence of the additional dispersion interactions by anions is very limited. The selected cations, on the other hand, present a higher variability in the interactions they can establish, and therefore, in their affinity. This was already observed in other computational studies in the literature, with a different theoretical approach [17].

4. Conclusion

This work presents a thorough description of the solvation of a lignin model in [BMIM][Cl], clarifying some controversial aspects of the process,

thanks to a multiscale approach. While consensus on the role of the anion exists, the role of the cation is particularly challenging due to the nature of the interaction it establishes. In this work, we have seen that AIMD simulations might be necessary if these interactions are to be captured adequately.

Our results reflect the role of imidazolium side chain when interacting with the lignin ring, discarding a π-π interaction between both rings, and consequently achieving agreement with experimental results regarding the role of imidazolium cation side chain, for the first time to the best of our knowledge [17, 18, 19]. Besides, our AIMD calculations captured a structuration of the imidazolium ring acidic hydrogen around the hydroxyl oxygen of the lignin, based on dispersion interactions. Summarizing, our results strongly suggest that the cation plays an important role in the solvation of lignin in stabilizing the aromatic ring with the alkyl chain, and the hydroxyl oxygen with the cation ring. Interactions with the hydroxyl group are specially relevant for the depolimerization process of lignin, which often begins with its dehydration [44].

Both findings are in line with previous theoretical and experimental studies on the microheterogeneity of ILs and their ability to act as structure-directing solvents [40, 41, 42, 43]: they report that ILs are microheterogeneous liquids where polar and apolar parts of the system are in separated domains, and act similarly when solvating molecules with a polar and an apolar part. The fact that it is the alkyl chain of the cation that solvates the lignin ring, and the acidic proton of the charged imidazolium ring is stabilizing the hydroxyl group of the solute is in perfect agreement with this description of the ILs.

Interestingly, our static DFT approach points out that the affinity of the IL towards the lignin may be ultimately determined by the cation, given that the anion establishes a sufficiently strong interaction with the hydroxyl, as previously suggested in the literature [17]. On this regard, choline cation based ILs seem particularly promising, since, besides dispersion interactions, these cations can create a hydrogen bond with the hydroxyl oxygen of the lignin, providing a further stabilization of this functional group.

Acknowledgements

We acknowledge the Basque Government - Eusko Jaurlaritza for financial support (projects IT1254-19 and ELKARTEK KK-2018/00102) and the

SGi/IZO-SGIker UPV/EHU for generous allocation of computational resources.

References

[1] X. Zhu, C. Peng, H. Chen, Q. Chen, Z. K. Zhao, Q. Zheng, and H. Xie, "Opportunities of Ionic Liquids for Lignin Utilization from Biorefinery," *ChemistrySelect*, vol. 3, no. 27, pp. 7945–7962, 2018.

[2] B. Lindner, L. Petridis, R. Schulz, and J. C. Smith, "Solvent-Driven Preferential Association of Lignin with Regions of Crystalline Cellulose in Molecular Dynamics Simulation," *Biomacromolecules*, vol. 14, no. 10, pp. 3390–3398, 2013. [Online]. Available: http://pubs.acs.org/doi/10.1021/bm400442n

[3] A. Brandt, J. Gräsvik, J. P. Hallett, and T. Welton, "Deconstruction of lignocellulosic biomass with ionic liquids," *Green Chemistry*, vol. 15, no. 3, p. 550, 2013. [Online]. Available: http://xlink.rsc.org/?DOI=c2gc36364j

[4] S. K. Singh, "Solubility of lignin and chitin in ionic liquids and their biomedical applications," *International Journal of Biological Macromolecules*, vol. 132, pp. 265–277, 2019. [Online]. Available: https://doi.org/10.1016/j.ijbiomac.2019.03.182

[5] F. S. Chakar and A. J. Ragauskas, *Industrial crops and products.* Elsevier Science, 2004, vol. 20, no. 2. [Online]. Available: https://www.cabdirect.org/cabdirect/abstract/20043188443

[6] A. M. da Costa Lopes, K. G. João, A. R. C. Morais, E. Bogel-Łukasik, and R. Bogel-Łukasik, "Ionic liquids as a tool for lignocellulosic biomass fractionation," *Sustainable Chemical Processes*, vol. 1, no. 1, p. 3, 2013. [Online]. Available: http://sustainablechemicalprocesses.springeropen.com/articles/10.1186/2043-7129-1-3

[7] A. T. Adeleye, H. Louis, H. A. Temitope, M. Philip, P. I. Amos, T. O. Magu, A. U. Ozioma, and O. O. Amusan, "Asian Journal of Green Chemistry Review Article Ionic liquids (ILs): advances in biorefinery for the efficient conversion of lignocellulosic biomass," vol. 3, pp. 391–417, 2019.

[8] K. Saha, P. Dwibedi, A. Ghosh, J. Sikder, S. Chakraborty, and S. Curcio, "Extraction of lignin, structural characterization and bioconversion of sugarcane bagasse after ionic liquid assisted pretreatment," *3 Biotech*, vol. 8, no. 8, pp. 1–12, 2018. [Online]. Available: http://dx.doi.org/10.1007/s13205-018-1399-4

[9] H. Wang, G. Gurau, and R. D. Rogers, "Ionic liquid processing of cellulose," *Chemical Society Reviews*, vol. 41, no. 4, p. 1519, 2012. [Online]. Available: http://xlink.rsc.org/?DOI=c2cs15311d

[10] Q. Zhang, J. Hu, and D.-j. Lee, "Pretreatment of biomass using ionic liquids : Research updates," *Renewable Energy*, vol. 111, pp. 77–84, 2017. [Online]. Available: http://dx.doi.org/10.1016/j.renene.2017.03.093

[11] O. Merino, G. Fundora-Galano, R. Luque, and R. Martínez-Palou, "Understanding microwave-assisted lignin solubilization in protic ionic liquids with multiaromatic imidazolium cations," *ACS Sustainable Chemistry & Engineering*, vol. 6, no. 3, pp. 4122–4129, 2018.

[12] B. G. Janesko, "Modeling interactions between lignocellulose and ionic liquids using dft-d," *Physical Chemistry Chemical Physics*, vol. 13, no. 23, pp. 11 393–11 401, 2011.

[13] ——, "Acid-catalyzed hydrolysis of lignin β-O-4 linkages in ionic liquid solvents: a computational mechanistic study," *Physical Chemistry Chemical Physics*, vol. 16, no. 11, pp. 5432–5433, 2014.

[14] N. Sun, R. Parthasarathi, A. M. Socha, J. Shi, S. Zhang, V. Stavila, K. L. Sale, B. A. Simmons, and S. Singh, "Understanding pretreatment efficacy of four cholinium and imidazolium ionic liquids by chemistry and computation," *Green Chemistry*, vol. 16, no. 5, pp. 2546–2557, 2014.

[15] V. S. Bernales, A. V. Marenich, R. Contreras, C. J. Cramer, and D. G. Truhlar, "Quantum Mechanical Continuum Solvation Models for Ionic Liquids," *The Journal of Physical Chemistry B*, vol. 116, no. 30, pp. 9122–9129, 2012. [Online]. Available: http://pubs.acs.org/doi/10.1021/jp304365v

[16] A. George, K. Tran, T. J. Morgan, P. I. Benke, C. Berrueco, E. Lorente, B. C. Wu, J. D. Keasling, B. A. Simmons, and B. M. Holmes, "The effect

of ionic liquid cation and anion combinations on the macromolecular structure of lignins," *Green Chemistry*, vol. 13, no. 12, p. 3375, 2011. [Online]. Available: http://xlink.rsc.org/?DOI=c1gc15543a

[17] W. Ji, Z. Ding, J. Liu, Q. Song, X. Xia, H. Gao, H. Wang, and W. Gu, "Mechanism of lignin dissolution and regeneration in ionic liquid," *Energy & Fuels*, vol. 26, no. 10, pp. 6393–6403, 2012.

[18] P. Moyer, M. D. Smith, N. Abdoulmoumine, S. C. Chmely, J. C. Smith, L. Petridis, and N. Labbé, "Relationship between lignocellulosic biomass dissolution and physicochemical properties of ionic liquids composed of 3-methylimidazolium cations and carboxylate anions," *Physical Chemistry Chemical Physics*, vol. 20, no. 4, pp. 2508–2516, 2018.

[19] S. H. Lee, T. V. Doherty, R. J. Linhardt, and J. S. Dordick, "Ionic liquid-mediated selective extraction of lignin from wood leading to enhanced enzymatic cellulose hydrolysis," *Biotechnology and Bioengineering*, vol. 102, no. 5, pp. 1368–1376, 2009. [Online]. Available: http://doi.wiley.com/10.1002/bit.22179

[20] I. Kilpeläinen, H. Xie, A. King, M. Granstrom, S. Heikkinen, and D. S. Argyropoulos, "Dissolution of Wood in Ionic Liquids," *Journal of Agricultural and Food Chemistry*, vol. 55, no. 22, pp. 9142–9148, 2007. [Online]. Available: https://pubs.acs.org/doi/10.1021/jf071692e

[21] Y. Zhu, J. Yan, C. Liu, and D. Zhang, "Modeling interactions between a β-O-4 type lignin model compound and 1-allyl-3-methylimidazolium chloride ionic liquid," *Biopolymers*, vol. 107, no. 8, p. e23022, 2017. [Online]. Available: http://doi.wiley.com/10.1002/bip.23022

[22] D. A. Fort, R. C. Remsing, R. P. Swatloski, P. Moyna, G. Moyna, and R. D. Rogers, "Can ionic liquids dissolve wood? Processing and analysis of lignocellulosic materials with 1-n-butyl-3-methylimidazolium chloride," *Green Chem.*, vol. 9, no. 1, pp. 63–69, 2007. [Online]. Available: http://xlink.rsc.org/?DOI=B607614A

[23] K. A. Underkofler, R. E. Teixeira, S. A. Pietsch, K. G. Knapp, and R. T. Raines, "Separation of Lignin from Corn Stover Hydrolysate with Quantitative Recovery of Ionic Liquid," *ACS Sustainable Chemistry*

461 *& Engineering*, vol. 3, no. 4, pp. 606–613, 2015. [Online]. Available:
462 http://pubs.acs.org/doi/10.1021/sc500731c

463 [24] E. Rezabal and T. Schäfer, "First principle approach to solvation by
464 methylimidazolium-based ionic liquids," *Journal of Physical Chemistry*
465 *B*, vol. 117, no. 2, 2013.

466 [25] E. Rezabal and T. Schäfer, "Ionic liquids as solvents of polar and non-
467 polar solutes: affinity and coordination," *Physical Chemistry Chemical*
468 *Physics*, vol. 17, no. 22, pp. 14 588–14 597, 2015.

469 [26] U. Domańska and L. Mazurowska, "Solubility of 1,3-dialkylimidazolium
470 chloride or hexafluorophosphate or methylsulfonate in organic sol-
471 vents: effect of the anions on solubility," *Fluid Phase Equi-*
472 *libria*, vol. 221, no. 1-2, pp. 73–82, 2004. [Online]. Available:
473 https://www.sciencedirect.com/science/article/pii/S0378381204001608

474 [27] S. Plimpton, "Fast parallel algorithms for short-range molecular dynam-
475 ics," *J. Comput. Phys.*, vol. 117, no. 1, pp. 1–19, 1995.

476 [28] W. L. Jorgensen, D. S. Maxwell, and J. Tirado-Rives, "Development
477 and testing of the opls all-atom force field on conformational energetics
478 and properties of organic liquids," *Journal of the American Chemical*
479 *Society*, vol. 118, no. 45, pp. 11 225–11 236, 1996.

480 [29] A. Mondal and S. Balasubramanian, "Quantitative Prediction of
481 Physical Properties of Imidazolium Based Room Temperature Ionic
482 Liquids through Determination of Condensed Phase Site Charges:
483 A Refined Force Field," *The Journal of Physical Chemistry*
484 *B*, vol. 118, no. 12, pp. 3409–3422, 2014. [Online]. Available:
485 http://pubs.acs.org/doi/10.1021/jp500296x

486 [30] L. Martínez, R. Andrade, E. G. Birgin, and J. M. Martínez, "Pack-
487 mol: a package for building initial configurations for molecular dynamics
488 simulations," *Journal of computational chemistry*, vol. 30, no. 13, pp.
489 2157–2164, 2009.

490 [31] R. W. Hockney and J. W. Eastwood, *Computer simulation using parti-*
491 *cles*. CRC Press, 1988.

[32] M. Parrinello and A. Rahman, "Polymorphic transitions in single crystals: A new molecular dynamics method," *Journal of Applied physics*, vol. 52, no. 12, pp. 7182–7190, 1981.

[33] "Open source molecular dynamics." [Online]. Available: https://www.cp2k.org/

[34] A. D. Becke, "Density-functional exchange-energy approximation with correct asymptotic-behavior," *Phys. Rev.*, vol. 38, no. 6, pp. 3098–3100, 1988.

[35] C. Lee, W. Yang, and R. G. Parr, "Development of the Colle-Salvetti correlation-energy formula into a functional of the electron density," *Phys. Rev. B*, vol. 37, no. 2, pp. 785–789, 1988.

[36] B. Miehlich, A. Savin, H. Stoll, and H. Preuss, "Results obtained with the correlation energy density functionals of becke and Lee, Yang and Parr," *Chem. Phys. Lett.*, vol. 157, no. 3, pp. 200–206, 1989.

[37] S. Grimme, T. O. Chemie, and O.-c. I. D. U. Münster, "Semiempirical GGA-Type Density Functional Constructed with a Long-Range Dispersion Correction," *J. Comput. Chem.*, vol. 27, pp. 1787–1799, 2006.

[38] J. VandeVondele and J. Hutter, "Gaussian basis sets for accurate calculations on molecular systems in gas and condensed phases," *The Journal of chemical physics*, vol. 127, no. 11, p. 114105, 2007.

[39] M. Brehm and B. Kirchner, "TRAVIS - A Free Analyzer and Visualizer for Monte Carlo and Molecular Dynamics Trajectories," *Journal of Chemical Information and Modeling*, vol. 51, no. 8, pp. 2007–2023, 2011. [Online]. Available: https://pubs.acs.org/doi/10.1021/ci200217w

[40] J. Contreras-Garcia, E. R. Johnson, S. Keinan, R. Chaudret, J.-P. Piquemal, D. N. Beratan, and W. Yang, "NCIPLOT: A Program for Plotting Noncovalent Interaction Regions," *J. Chem. Theory Comput.*, vol. 7, no. 3, pp. 625–632, 2011.

[41] E. R. Johnson, S. Keinan, P. Mori-Sanchez, J. Contreras-Garcia, A. J. Cohen, and W. Yang, "Revealing Noncovalent Interactions," *J. Am. Chem. Soc.*, vol. 132, no. 18, pp. 6498–6506, 2010.

[42] M. J. Frisch, G. W. Trucks, H. B. Schlegel, G. E. Scuseria, M. A. Robb, J. R. Cheeseman, G. Scalmani, V. Barone, B. Mennucci, G. A. Petersson, H. Nakatsuji, M. Caricato, X. Li, H. P. Hratchian, A. F. Izmaylov, J. Bloino, G. Zheng, J. L. Sonnenberg, M. Hada, M. Ehara, K. Toyota, R. Fukuda, J. Hasegawa, M. Ishida, T. Nakajima, Y. Honda, O. Kitao, H. Nakai, T. Vreven, J. A. Montgomery Jr., J. E. Peralta, F. Ogliaro, M. Bearpark, J. J. Heyd, E. Brothers, K. N. Kudin, V. N. Staroverov, R. Kobayashi, J. Normand, K. Raghavachari, A. Rendell, J. C. Burant, S. S. Iyengar, J. Tomasi, M. Cossi, N. Rega, J. M. Millam, M. Klene, J. E. Knox, J. B. Cross, V. Bakken, C. Adamo, J. Jaramillo, R. Gomperts, R. E. Stratmann, O. Yazyev, A. J. Austin, R. Cammi, C. Pomelli, J. W. Ochterski, R. L. Martin, K. Morokuma, V. G. Zakrzewski, G. A. Voth, P. Salvador, J. J. Dannenberg, S. Dapprich, A. D. Daniels, Ö. Farkas, J. B. Foresman, J. V. Ortiz, J. Cioslowski, and D. J. Fox, "Gaussian09 {R}evision {D}.01."

[43] P. J. Stephens, F. J. Devlin, C. F. Chabalowski, and M. J. Frisch, "Ab Initio Calculation of Vibrational Absorption and Circular Dichroism Spectra Using Density Functional Force Fields," *The Journal of Physical Chemistry*, vol. 98, no. 45, pp. 11 623–11 627, 1994. [Online]. Available: http://pubs.acs.org/doi/abs/10.1021/j100096a001

[44] A. Schafer, H. Horn, and R. Ahlrichs, "Fully optimized contracted Gaussian basis sets for atoms Li to Kr," *The Journal of Chemical Physics*, vol. 97, no. 4, pp. 2571–2577, 1992. [Online]. Available: http://link.aip.org/link/?JCP/97/2571/1

[45] S. Grimme, W. Hujo, and B. Kirchner, "Performance of dispersion-corrected density functional theory for the interactions in ionic liquids," *Phys. Chem. Chem. Phys.*, vol. 14, no. 14, pp. 4875–4883, 2012.

[46] Y. Zhao and D. G. Truhlar, "The m06 suite of density functionals for main group thermochemistry, thermochemical kinetics, noncovalent interactions, excited states, and transition elements: two new functionals and systematic testing of four m06-class functionals and 12 other functionals," *Theoretical Chemistry Accounts*, vol. 120, no. 1-3, pp. 215–241, 2008.

[47] A. Schafer, C. Huber, and R. Ahlrichs, "Fully optimized contracted Gaussian basis sets of triple zeta valence quality for atoms Li to Kr,"

The Journal of Chemical Physics, vol. 100, no. 8, pp. 5829–5835, 1994. [Online]. Available: http://link.aip.org/link/?JCP/100/5829/1

[48] N. Sun, M. Rahman, Y. Qin, M. L. Maxim, H. Rodríguez, and R. D. Rogers, "Complete dissolution and partial delignification of wood in the ionic liquid 1-ethyl-3-methylimidazolium acetate," *Green Chemistry*, vol. 11, no. 5, pp. 646–655, 2009.

[49] Y. Zhang, F. Huo, Y. Wang, Y. Xia, X. Tan, S. Zhang, and H. He, "Theoretical Elucidation of β-O-4 Bond Cleavage of Lignin Model Compound Promoted by Sulfonic Acid-Functionalized Ionic Liquid," *Frontiers in Chemistry*, vol. 7, no. February, 2019.

[50] R. Elfgen, O. Hollóczki, and B. Kirchner, "A Molecular Level Understanding of Template Effects in Ionic Liquids," *Accounts of Chemical Research*, vol. 50, no. 12, pp. 2949–2957, 2017. [Online]. Available: http://pubs.acs.org/doi/10.1021/acs.accounts.7b00436

[51] A. Triolo, O. Russina, H.-J. Bleif, and E. Di Cola, "Nanoscale segregation in room temperature ionic liquids," *The Journal of Physical Chemistry B*, vol. 111, no. 18, pp. 4641–4644, 2007.

[52] J. J. Hettige, H. K. Kashyap, H. V. R. Annapureddy, and C. J. Margulis, "Anions, the Reporters of Structure in Ionic Liquids," *The Journal of Physical Chemistry Letters*, vol. 4, no. 1, pp. 105–110, 2013. [Online]. Available: http://pubs.acs.org/doi/10.1021/jz301866f

[53] J. J. Hettige, J. C. Araque, and C. J. Margulis, "Bicontinuity and Multiple Length Scale Ordering in Triphilic Hydrogen-Bonding Ionic Liquids," *The Journal of Physical Chemistry B*, vol. 118, no. 44, pp. 12 706–12 716, 2014. [Online]. Available: http://pubs.acs.org/doi/10.1021/jp5068457